PERIODICO di MINERALOGIA
established in 1930

An International Journal of
Mineralogy, Crystallography, Geochemistry,
Ore Deposits, Petrology, Volcanology
and applied topics on Environment, Archaeometry and Cultural Heritage

Dipartimento
di Scienze della Terra
Sapienza
Università di Roma

Mineralogy and petrology of the metasedimentary rocks from the Frido Unit (southern Apennines, Italy)

Giovanna Rizzo[1,*], Maria Teresa Cristi Sansone[1], Francesco Perri[2], Salvatore Laurita[1]

[1] Università degli Studi della Basilicata, Dipartimento di Scienze, Potenza, Italy
[2] Università della Calabria, Dipartimento di Biologia Ecologia e Scienze della Terra, Rende (CS)

ARTICLE INFO

Submitted: February 2016
Accepted: May 2016
Available on line: May 2016

* Corresponding author:
giovanna.rizzo@unibas.it

DOI: 10.2451/2016PM630

How to cite this article:
Rizzo G. et al. (2016) Period. Mineral. 85, 153-168

ABSTRACT

This work concerns the development of a multidisciplinary research on metasedimentary rocks from the Frido Unit (southern Apennines) in the central Mediterranean area, based on petrographic study, mineralogical analysis and distribution of the major and trace elements. It aims at evaluating the paleoweathering conditions and provenance composition of the source area(s) of both shales and calcschists from the Frido Unit. Shales and calcschists underwent similar HP/LT overprint, by the occurrence of aragonite, as also shown by mineralogical analysis. The mineralogical composition of the studied rocks closely related to the geochemical variations, as shown by the negative correlation of CaO with other elements, due to the dilution effects by the carbonates, and the positive correlation of Al with most of the major and trace elements mainly related to the mica-like clay minerals. Elemental ratios, such as the Chemical Index of Alteration (CIA) and the Index of Compositional Variability (ICV), indicate low to moderate degree of chemical weathering at relatively immature source area(s) and, thus, first-cycle deposits related to tectonically active settings. Furthermore, the distribution of some major and trace elements suggest provenance for the studied samples from source(s) composed of both felsic and mafic rocks.

Keywords: metasedimentary rocks; petrography; geochemistry; mineralogy; Frido Unit; southern Apennines.

INTRODUCTION

The Frido Unit rocks (Vezzani, 1969) belonging to the Liguride Complex in the southern Apennines, derived from paleogeographic domains of the Jurassic Neothetys ocean (Stampfli et al., 2002; Tortorici et al., 2009) that separated the European and African continental margin.

In the central Mediterranean area, an Apulian microplate is generally identified north of the African plate. This may be separated into an Apulian part to the south, representing an African promontory, and an Adriatic part to the north, which may be seen as an independent microplate in the Cretaceous-Late Eocene time interval (Stampfli et al., 2002; Schettino and Turco, 2011; Laurita et al., 2014).

The Frido Unit consists essentially of shales, calcschists, and metalimestones with associated ophiolites (Monaco and Tortorici, 1995). Slivers of continental crust (Spadea, 1982; Knott, 1987; 1994; Monaco et al., 1995; Monaco and Tortorici, 1995; Tortorici et al., 2009) occur as a thrust fault delimiting the upper portion of this unit from a lower portion.

According to Cavalcante et al. (2012), phyllosilicates in metasediments indicate that the Frido Unit was subjected to variable pressure and temperatures overprint. Furthermore, the preservation of aragonite indicates that different thrust sheets of the Frido Unit underwent fast exhumation after the pressure and temperature peak in the accretionary wedge (Cavalcante et al., 2012).

The occurrence of white mica and chlorite (in phyllites and metapelites of the Frido Unit), indicates a HP/VLT metamorphism characterized by pressures of ~1.2-1.4 GPa and temperatures around 350 °C (Vitale et al., 2013).

This study reports new petrographic, geochemical and mineralogical analyses of the metasedimentary rocks of the Frido Unit. The geochemical proxies coupled to petrographic and mineralogical analyses provide useful information on the geological processes, source area provenance and tectonic setting of the studied metasedimenty rocks (Cullers et al., 1979; 1987; 1988; Taylor and McLennan, 1985; Cullers and Stone, 1991; McLennan et al., 1993; Perri et al., 2013, 2016; El Talibi et al., 2014; Perri, 2014; Perri and Ohta, 2014). Therefore, it is possible to better understand the effects of the geological processes on the petrographic, geochemical and mineralogical signatures of the Frido Unit metasedimentary rocks in the central Mediterranean area.

GEOLOGICAL SETTING

The southern Apennines are a NW-SE oriented segment of the Apennine fold and-thrust belt developed between the Upper Oligocene and the Quaternary times during the convergence between the Adria and European plates and closure of the Tethyan ocean with the simultaneous roll-back to SE of the Ionian subducted slab (Gueguen et al., 1998; Cello and Mazzoli, 1999; Critelli 1999; Doglioni et al., 1999; Patacca and Scandone, 2007). According to some authors (Ogniben, 1969; Knott, 1987; 1994; Monaco et al., 1991; Tortorici et al., 2009), the Liguride Complex in the southern Apennines represents the suture zone between the converging Europe and Adria plates. The development of the accretionary wedge took place during Cretaceous-Pleogene to Oligocene time (Knott, 1994; Cello and Mazzoli, 1999).

The Liguride Complex allochthonous successions constitute the highest units in the Apennine chain (Figure 1 a,b). According to Bonardi et al. (1988), these units consist of the Frido Unit, the Episcopia-San Severino Mélange, the Northern Calabrian Unit and the Sicilian-type terranes. The former three units have oceanic origin, whilst the fourth has a continental nature (Bonardi et al., 2009). The Frido Unit blocks of various size made up of ophiolites and continental crustal rocks (Spadea, 1982).

Monaco and Tortorici (1995) divided the Frido Units into a lower sub-unit mainly consisting of shales, and an upper sub-unit made up of calcschists. In the geological map of the north-eastern side of Pollino Massif (Monaco et al. 1995) the serpentinites occur only sporadically along the contact. Serpentinites mostly consist of cataclastic rocks, with some metabasalt dikes and rodingite (Sansone et al., 2012b; Sansone and Rizzo, 2009; 2010).

The shales of the lower sub-unit show grey- and/or black colour, with intercalation of metarenites, quartzite and rare levels of metalimestones of oldest Upper Cretaceous age (Vezzani, 1969). The shales show schistose structure and advanced penetrative deformation that obliterated the primary foliation (S_0). The deformation (S_1) consists of slaty cleavage, crenulation cleavage and isoclinalic fold with limbs lying parallel to bedding (bedding-parallel foliation) (Knott, 1987; 1994). Metarenitic levels show boudinage as pinch and swell structure. Small veins crack-seal type filled by quartz, and/or calcite are observed, and aragonite (Spadea, 1976; Monaco et al., 1991; Cirrincione and Monaco, 1996).

The upper sub-unit of calcschists consists of limestone and marble with variable thickness. They are crosscut by veins filled by calcite. Intercalations consist of rare levels of marbles, greenish quartzites, black fine-grained shales macroscopically similar to those of the lower subunit. The maximum thickness is estimated at several hundred meters (Vezzani, 1969; Monaco et al., 1991). The calcschists are characterized by marked planar anisotropy, highlighted by the orientation of phyllosilicate minerals (Monaco et al., 1991).

The Frido Unit shows ocean-floor metamorphism under amphibolite to greenschist facies conditions (Monaco et al., 1995; Cirrincione and Monaco, 1996; Piluso et al., 2000; Spadea, 1994; Sansone et al., 2011; 2012a; Sansone and Rizzo, 2012). The subsequent subduction related metamorphism under relatively HP/LT (blueschist facies) conditions affected the rocks during the formation of the Apennine accretionary prism (Cello and Mazzoli, 1999; Sansone et al., 2011; Sansone et al., 2012a).

The Frido Unit ophiolites record physical conditions of the orogenic metamorphism that have been estimated to be at P=0.6-0.8 GPa and T=200-300 °C (Spadea, 1994; Sansone et al., 2011).

Similar conditions have been obtained by fluid inclusion studies conducted on some metasediments (Invernizzi et al., 2008), whereas thermobaric conditions of P=1.1-1.3 GPa and T=280-320 °C have been estimated by Cavalcante et al. (2009) for the metapelites from the southern Frido Unit. Notably, these latter rocks are different compared to the shales described above due to the fact that metapelites were sampled in different areas.

SAMPLING AND METHODS

Six samples of shales (according to Monaco and Tortorici, 1995) and six samples of calcschists from the Frido Unit were collected close to the San Severino Lucano village (southern Italy; Figure 1 a,b). Shales are grey and massive, with varying grain sizes and cross cut by carbonate veins structure arranged transversely and sub-parallel to the main foliation (Figure 2a) and with ductile deformation. The minerals in the veins do not show metamorphic overprint. These veins were observed in beds of dark calcite and white calcite. Calcschists show sedimentary structures as parallel and oblique lamination. The main foliation is generally crenulated and affected by tight and isoclinal fold, (Figure 2b).

Preliminary petrographic characterization was carried out with an optical microscopy on oriented rock samples as

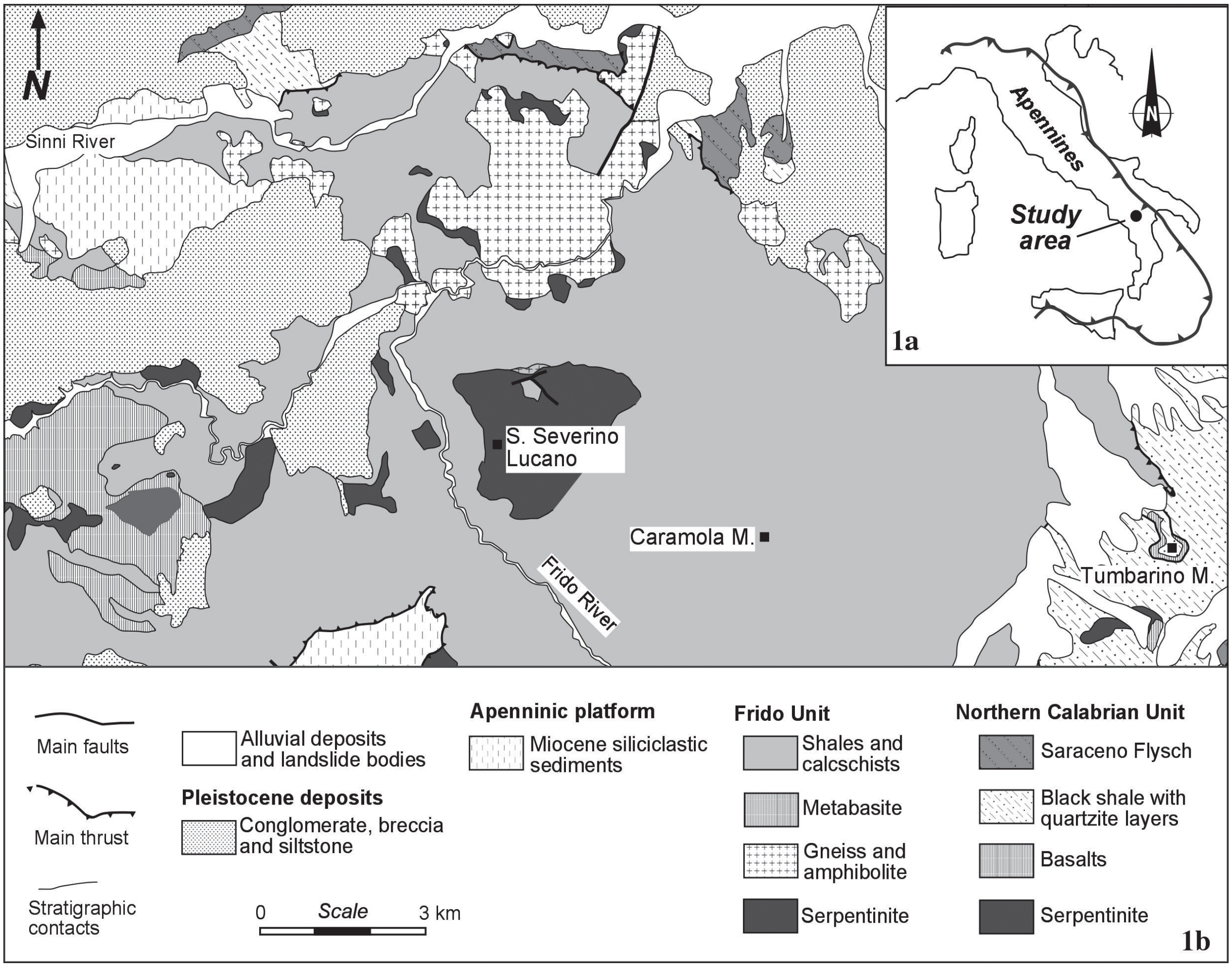

Figure 1. Geological sketch map of (a) the southern Apennines with the location of the study area and of (b) (modified from Laurita, 2009).

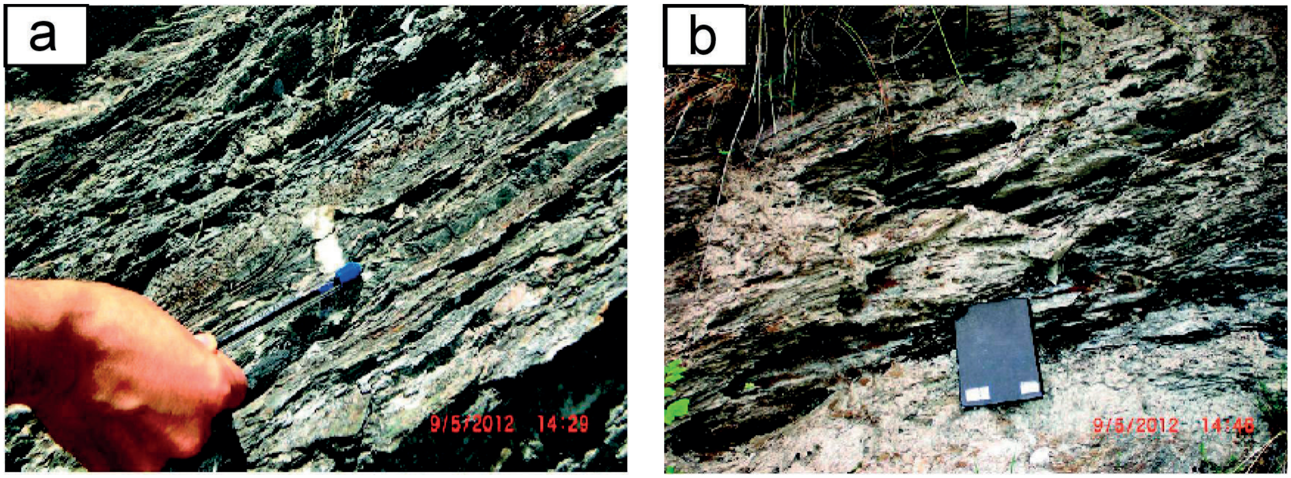

Figure 2. Exposure of key lithofacies of the shale (a) and calcschist (b) samples.

a function of their foliations and lineations.

The mineralogy of the whole-rock was determined by X-ray powder diffraction (XRD) using a Rigaku D/max 2200 diffractometer (Cu-Kα radiation; graphite secondary monochromator; sample spinner; step size 0.02; speed 3 sec step).

Quantitative mineralogical analysis of the bulk rock was performed on random powders measuring peak areas using WINFIT computer program (Krumm, 1996). The strongest reflection of each mineral was considered, except for quartz for which the line at 4.26 Å was used instead of the peak at 3.34 Å because of its superimposition with 10 Å-minerals and I-S mixed layer series (Cavalcante et al., 2007; Perri, 2008; Perri et al., 2008; 2011b; 2012b; 2016). The weight percentage of each mineral was obtained following the procedure proposed by Cavalcante et al. (2007).

Elemental analyses for major and some trace elements (Nb, Zr, Y, Sr, Rb, Ba, Ni, Co, Cu, Cr, V) were obtained by X-ray fluorescence spectrometry (Bruker S8 Tiger) at the University of Calabria (Italy), on pressed powder disks of whole-rock samples (prepared by milling to a fine grained powder in agate mill) and compared to international standard rock analyses of the United States Geological Survey. X-ray counts were converted into concentrations by a computer program based on the matrix correction method according to (Franzini et al., 1972; 1975) and (Leoni and Saitta, 1976). The loss on ignition (L.O.I.) was determined after heating the samples for 3 h at 900 °C. The estimated precision and accuracy for trace element determinations are better than 5%, except for those elements having concentration of 10 ppm or less (10-15%).

RESULTS

Petrography

Shales

Shales show cataclastic/mylonitic fabric. They are cut by veins filled with calcite, chlorite and quartz arranged transverse or sub-parallel to the planar anisotropy of rocks. Metamorphic minerals are white mica, chlorite, epidote. Relict minerals are plagioclase and calcite. Accessory minerals are Fe-hydroxides, opaque minerals, apatite and zircon.

The kinematic indicators as σ e δ and C'-S structure show the presence of extensional shear bands (Passchier

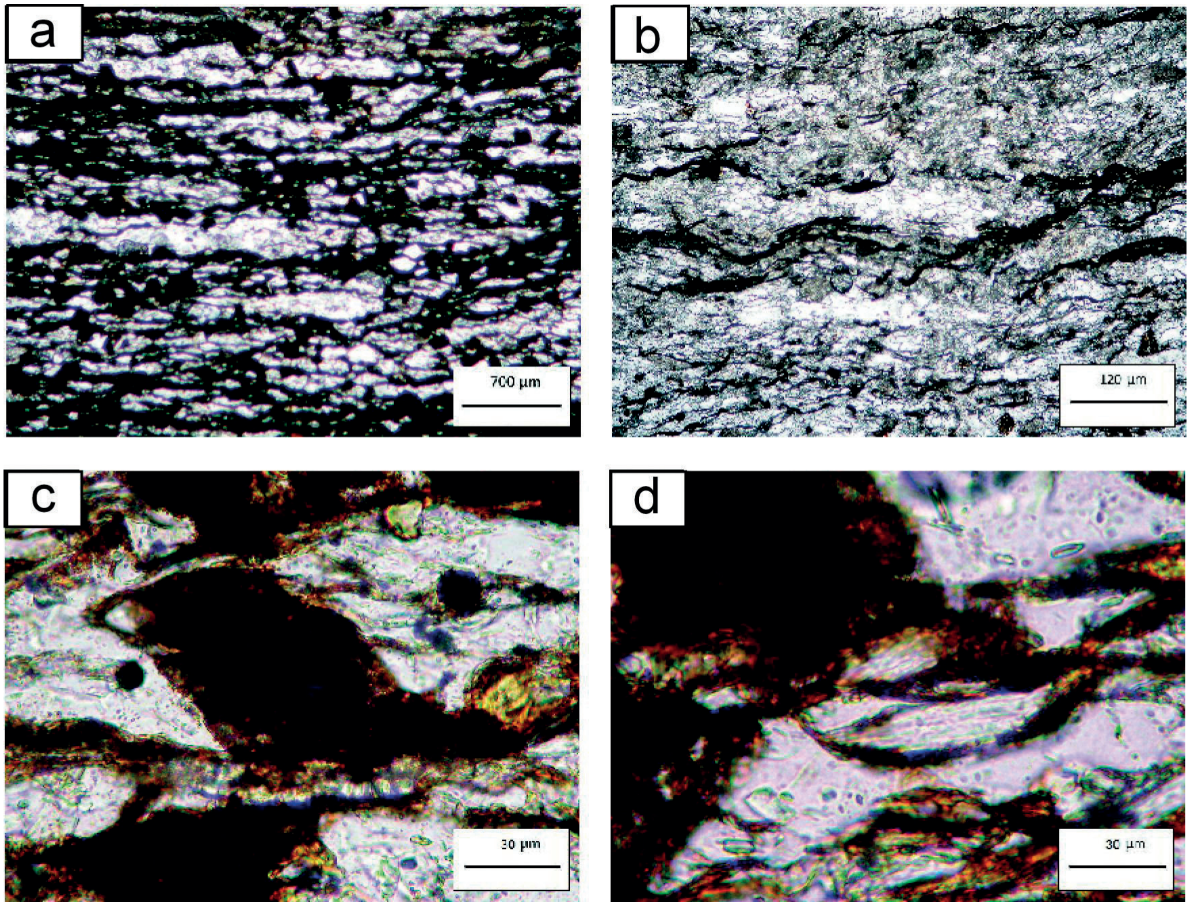

Figure 3. (a) Cataclastic/Mylonitic fabric; (b) crenulation cleavage domains defined by stilpnomelane; (c, d) porphyroclastic rutile and mica fish in the shale sample.

and Trouw, 2005) (Figure 3a). The foliation of the shales is characterized by crenulation cleavage domains defined by stilpnomelane (Figure 3b), white mica and quartz-rich levels constituting microlithons (Passchier and Trouw, 2005).

Porphyroclastic rutile is associated with mica fish of white mica crystals (Figure 3c) and sometimes located along the crenulation cleavage. Mantled porphyroclast rutile is consistent with a sinistral shear sense top to WNW. Single crystals of mica commonly have a lozenge shape (Passchier and Trouw, 2005) and shows stair stepping wings with a dextral shear sense (Figure 3d). Subidioblastic stilpnomelane crystals along the main schistosity and occasionally associated with white mica and chlorite in the cleavage domains. White mica crystals are associated with chlorite, stilpnomelane and rutile crystals.

Quartz shows an ondulose extinction, dynamic recrystallization as sub-grains, sometimes deformation bands. Chlorite occurs as single crystals or associated with quartz and white mica crystals.

Plagioclase subidioblastic crystals show deformation twins. Epidote forms aggregates with chlorite and exhibit pale-green pleochroism. Colourless crystals of calcite exhibit polysynthetic twinning and have a prismatic habit. Abundant Fe-hydroxides crystals, subidioblastic opaque minerals and zircons are found as inclusions in stilpnomelane. Anatase exsolution lamellae occur as pseudomorph after rutile.

Calcschists

Calcschists show cataclastic-mylonitic foliation. The mineral assemblage is composed of calcite, quartz, plagioclase, K-feldspar, chlorite, white mica and stilpnomelane. Accessory phases are opaque minerals, Fe-hydroxides and zircons. The phyllosilicates, as chlorite, white mica and stilpnomelane, characterize the main foliation of the calcschists (Figure 4 a,b).

Some samples have heteroblastic structure and contain fine recrystallized quartz grains (Passchier and Trouw, 2005) as new grains (Figure 4c).

Calcite have a subidioblastic habit. Colourless crystals of calcite exhibit polysynthetic twinning and deformation twins (Figure 4d), less than 1 μm wide. Quartz xenoblasts exhibit ondulose extinction. Some crystals are cut by veins filled by calcite. Plagioclase subidioblastic crystals

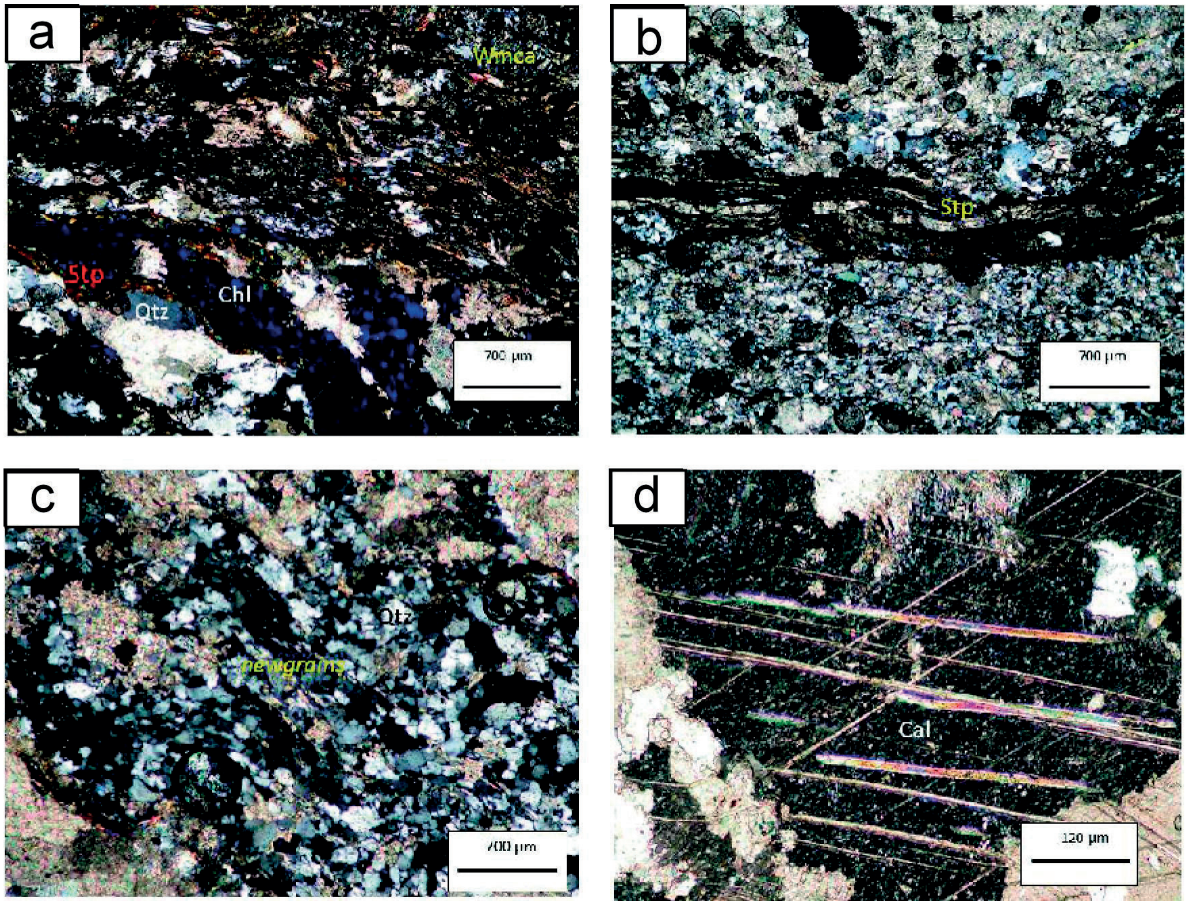

Figure 4. (a) Mylonitic foliation, (b) ductile deformation in stilpnomelane, (c) recrystallized quartz grains with new grains, (d) crystals of calcite with deformation twins in the calcschist samples.

have anortitic composition. Some crystals are completely sericitized. K-feldspar subidioblastic crystals have orthoclase composition. Chlorite are associated with other minerals such as white mica and stilpnomelane. White mica is present as idioblastic flakes and shows ductile deformation. Stilpnomelane occurs as lamellae and sometimes shows ductile deformation (Figure 4b). Stilpnomelane is usually associated with Fe-hydroxides, white mica and chlorite along the foliation. Rounded and elongate crystals of opaque minerals are present in the rocks. Prismatic zircon crystals are found as inclusions in stilpnomelane.

Metamorphic evolution of metasedimentary rocks

The Frido Unit shows several deformation events, in the shales characterized by LP/LT conditions, in the calcschists characterized by HP/LT conditions, developed during emplacement into the Liguride Complex.

In fact the shales of the Frido Unit are characterised by metamorphic conditions between anchimetamorfism and greenschist facies (Figure 5) according to previous authors (Di Leo et al., 2005; Cavalcante et al., 2012; Vitale et al., 2013).

The calcschists of the Frido Unit show greenschist indicates that these rocks were affected by HP/LT conditions (Figure 5). This is also consistent with data on the illite crystallinity and the b0 parameter of K-white mica in phyllites (Spadea, 1976; Cavalcante et al., 2012; Vitale et al., 2013). The presence of aragonite constrained the pressure peak around 0.8-1.0 GPa and ~400-450 °C temperature, with a subsequent requilibration at greenschist facies conditions (P~0.4 GPa and T~300-350 °C) (Monaco et al., 1991; Vitale et al., 2013).

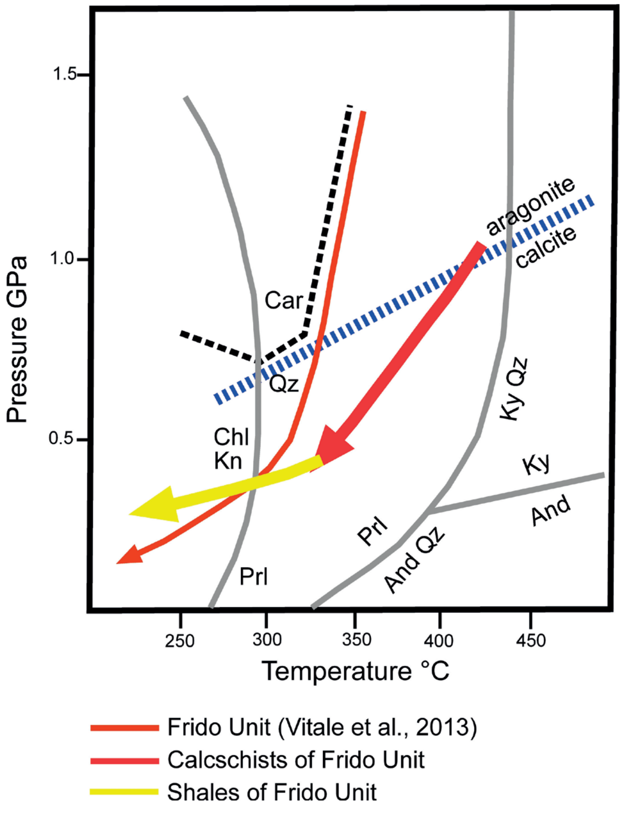

Figure 5. P–T paths for the Frido Units, calcschists of Frido Unit, shales of Frido Unit (modified after Vitale et al., 2013).

Mineralogical composition

The mineralogical assemblages of the studied samples are reported in Table 1. The non-phyllosilicate minerals are generally represented by quartz, carbonates (calcite and aragonite), feldspars (plagioclase and K-feldspar) and trace of hematite in some samples. The phyllosilicates are generally represented by chlorite, K-mica (illite-muscovite) and Na-mica (paragonite); I-S (illite-smectite) and Chl-S (chlorite-smectite) mixed layers are present in amounts.

In detail, the shale samples (AL) are mostly characterized by phyllosilicates whereas the calcschist samples (PG) mainly contain carbonate minerals (calcite is the most abundant phase) (Table 1).

The AL1, AL2 and AL3 samples show higher percentage of carbonate (mainly calcite and minor amounts of aragonite), ranging from 27% to 65%, and minor percentage of phyllosilicates, ranging from 10% to 12%, AL4, AL5 and AL6 samples (Table 1). The last samples are instead enriched in phyllosilicates, ranging from 24% to 43%, with minor amounts of calcite and aragonite, ranging from traces up to 4% (Table 1). The feldspars show higher concentrations in the AL4, AL5 and AL6 samples, ranging from 12% to 24%, rather than in AL1, AL2 and AL3 samples, ranging from 3% to 11% (Table 1). The AL3 sample is characterized by higher percentage of quartz compared to other samples, since it is enriched in quartz veins as also observed in the petrographic analysis. The PG3, PG4, PG5 and PG6 samples have higher percentage of carbonate (mainly calcite and minor amounts of aragonite), ranging from 58% to 71%, and minor percentage of quartz and feldspars for PG1 and PG2 samples, showing large amounts of quartz with values up to 58%, and feldspars with values up to 21% (Table 1). The phyllosicates percentage is higher in the PG3, PG4, PG5 and PG6 samples, ranging from 9% to 12%, rather than in the PG1 and PG2 samples characterized by values up to 7% (Table 1). In particular, the PG1 sample has a higher percentage of quartz.

Whole-rock geochemistry

The calcschist (PG) and the shale samples display distinctive geochemical characteristics, and their whole-rock major and trace element compositions are given in Table 2. To better examine the geochemical features of the studied samples, we normalize their composition to

Table 1. Mineralogical assemblage of the studied samples.

Sample	I/S	Chl/S	Illite and mica	Kln	Chl	Σ Phyll	Qtz	Σ Felds	Arag	Calc	Hem
AL1	tr	tr	4	0	7	11	22	6	5	56	0
AL2	tr	tr	4	0	8	12	20	3	5	60	tr
AL3	tr	tr	3	0	7	10	51	11	2	26	tr
AL4	1	tr	23	0	19	43	38	17	tr	1	tr
AL5	1	tr	16	0	18	35	48	12	tr	4	tr
AL6	1	tr	10	0	13	24	48	24	tr	3	tr
PG1	tr	tr	2	0	2	4	58	7	tr	30	tr
PG2	tr	tr	2	0	5	7	27	21	1	44	tr
PG3	tr	tr	5	0	4	9	18	6	1	65	0
PG4	tr	tr	5	0	5	9	18	3	4	66	0
PG5	tr	tr	6	0	4	10	24	6	tr	59	0
PG6	tr	tr	6	0	4	10	24	6	2	58	0

Legend: I/S=illite-smectite mixed layers; Chl/S=chlorite-smectite mixed layers; Kln=kaolinite; Chl=chlorite; Phyll=sum of phyllosilicates; Qtz=quartz; Felds=sum of feldspars; Arag=aragonite; Calc=calcite; Hem=hematite; tr=traces.

the upper continental crust (UCC; McLennan et al., 2006) (Figure 6).

The calcschist samples (PG) exhibit similar chemical variations relative to UCC (Figure 6a). These samples are depleted in Si, Ti, Al, Fe, Mg, Na, K and P relative to the UCC, and are enriched in Ca. Some samples are enriched in Mn, whereas others are depleted. Relative to the UCC, the samples are depleted in Ni, V, Co, Zn, Ba, Rb, Nb and Zr, and are enriched in Sr.

Cr shows enrichment, relative to the UCC, in PG1 and PG2, whereas shows depletion in PG3, PG4, PG5 and PG6. Cu shows enrichment relative to the UCC in PG4, PG5 and PG6, and depletion in PG1, PG2, and PG3. Y shows enrichment relative to the UCC in PG2, and depletion in PG1, PG3, PG4, PG5 and PG6.

Calcium and strontium share the same distribution over the entire whole-rock dataset, matching the distribution of $CaCO_3$-phases (calcite and aragonite) (Wasylenki et al., 2005; Bracco et al., 2012). Mg is depleted relative to the UCC, and is accompanied by the absence of dolomite in the carbonates.

Based on the chemical variations relative to UCC, the shale samples (AL) can be divided in two groups; the first group is composed by AL1, AL2 and AL3 samples, whereas the second group is composed by AL4, AL5 and AL6 samples characterized the second group (Figure 6b).

The first group is depleted in Si, Ti, Al, Fe, Mg, Na, K and P relative to the UCC, and is enriched in Ca. These samples are depleted in Ni, V, Co, Zn, Ba, Rb, Nb and Zr relative to the UCC, and are enriched in Sr and Cr.

The second group shows an opposite distribution. In particular, these samples are enriched in Ti, Al, Fe and Mg, relative to the UCC, and depleted in Ca, Na and P; Si and K showing similar concentration relative to the UCC. Among the trace elements, these samples are enriched in Ni, Cr, V, Co, Zn, Rb, Nb, Y and Zr relative to the UCC, and are depleted in Sr.

This opposite distribution between the first and the second group is mainly related to the different abundance of phyllosilicates and carbonates; in particular the first group (AL1, AL2 and AL3 samples) is characterized by higher content of $CaCO_3$-phases (calcite and aragonite) and lower content of phyllosilicates and feldspars the second group (AL1, AL2 and AL3 samples), as shown by mineralogical investigations.

Table 2. Major and trace element distribution and ratios of the studied samples.

	PG1	PG2	PG3	PG4	PG5	PG6	Mean	St. Dev.	Max	Mix	AL1	AL2	AL3	AL4	AL5	AL6	Mean	St. Dev.	Max	Mix
Oxides (wt%)																				
SiO_2	55.70	45.81	25.39	23.13	27.73	27.10	34.14	13.34	55.70	23.13	29.16	19.30	58.12	49.68	50.91	57.50	44.11	16.07	58.12	19.30
TiO_2	0.23	0.19	0.18	0.07	0.14	0.18	0.16	0.06	0.23	0.07	0.16	0.20	0.26	1.20	1.04	1.02	0.65	0.49	1.20	0.16
Al_2O_3	4.27	2.90	3.45	1.52	3.15	3.47	3.13	0.91	4.27	1.52	3.53	4.22	5.09	23.30	19.70	18.45	12.38	9.03	23.30	3.53
Fe_2O_3	3.03	2.08	1.95	1.77	1.99	1.66	2.08	0.49	3.03	1.66	1.65	3.78	3.03	9.31	9.56	7.20	5.75	3.39	9.56	1.65
MnO	0.07	0.16	0.07	0.07	0.08	0.13	0.09	0.04	0.16	0.07	0.05	0.16	0.08	0.11	0.19	0.20	0.13	0.06	0.20	0.05
MgO	1.17	0.82	1.24	0.72	1.06	0.86	0.98	0.21	1.24	0.72	0.82	1.63	1.36	3.51	3.53	2.91	2.29	1.17	3.53	0.82
CaO	17.93	25.99	38.21	40.27	33.85	35.01	31.88	8.41	40.27	17.93	34.73	36.73	16.33	1.02	3.03	2.30	15.69	16.50	36.73	1.02
Na_2O	0.59	0.24	0.06	0.02	0.07	0.10	0.18	0.22	0.59	0.02	0.08	0.00	0.25	1.42	1.12	1.67	0.76	0.73	1.67	0.00
K_2O	0.55	0.52	0.72	0.28	0.64	0.82	0.59	0.19	0.82	0.28	0.91	0.83	0.78	3.90	3.19	2.91	2.09	1.40	3.90	0.78
P_2O_5	0.05	0.04	0.05	0.05	0.06	0.07	0.05	0.01	0.07	0.04	0.03	0.07	0.04	0.13	0.10	0.12	0.08	0.04	0.13	0.03
L.O.I.	16.30	21.05	28.32	32.02	31.04	30.22	26.49	6.35	32.02	16.30	28.15	33.12	14.23	6.17	7.44	5.29	15.73	12.07	33.12	5.29
Total	99.90	99.80	99.63	99.91	99.81	99.62	99.78	0.13	99.91	99.62	99.27	100.04	99.57	99.76	99.79	99.56	99.66	0.26	100.04	99.27
Trace elements (ppm)																				
Ni	18	11	14	10	13	12	13	3	18	10	10	16	21	70	73	60	42	29	73	10
Cr	488	205	57	52	55	74	155	173	488	52	195	48	222	176	152	164	160	60	222	48
V	36	24	31	13	29	33	28	8	36	13	34	44	34	193	152	124	97	69	193	34
Co	10	7	2	2	2	2	4	3	10	2	2	2	8	38	30	23	17	15	38	2
Cu	20	21	20	32	32	34	26	7	34	20	28	41	21	39	36	28	32	8	41	21
Zn	41	25	41	24	45	28	34	9	45	24	30	56	44	133	124	110	83	45	133	30
Ba	56	42	70	69	68	91	66	16	91	42	67	59	83	477	377	283	224	180	477	59
Sr	1160	1787	2134	2413	1905	2472	1979	483	2472	1160	3704	2916	1433	39	82	48	1370	1614	3704	39
Rb	24	22	31	12	29	37	26	9	37	12	32	33	31	210	169	135	102	80	210	31
Nb	3	3	2	2	3	2	3	1	3	2	2	2	4	22	19	17	11	9	22	2
Y	19	27	19	16	18	16	19	4	27	16	16	19	17	27	30	31	23	7	31	16
Zr	119	126	78	66	66	96	92	26	126	66	130	99	165	194	170	233	165	47	233	99
Ratios																				
CIA	60.24	56.89	57.97	56.82	59.00	56.11	57.84	1.55	60.24	56.11	64.71	70.69	67.63	73.64	73.15	71.52	70.22	3.44	73.64	64.71
CIA’	71.74	71.80	74.04	76.52	74.02	70.96	73.18	2.08	76.52	70.96	69.64	76.39	76.44	74.21	75.04	72.81	74.09	2.58	76.44	69.64
ICV	5.50	10.27	12.26	28.38	11.98	11.15	13.26	7.81	28.38	5.50	10.87	10.24	4.33	0.87	1.09	0.98	4.73	4.70	10.87	0.87

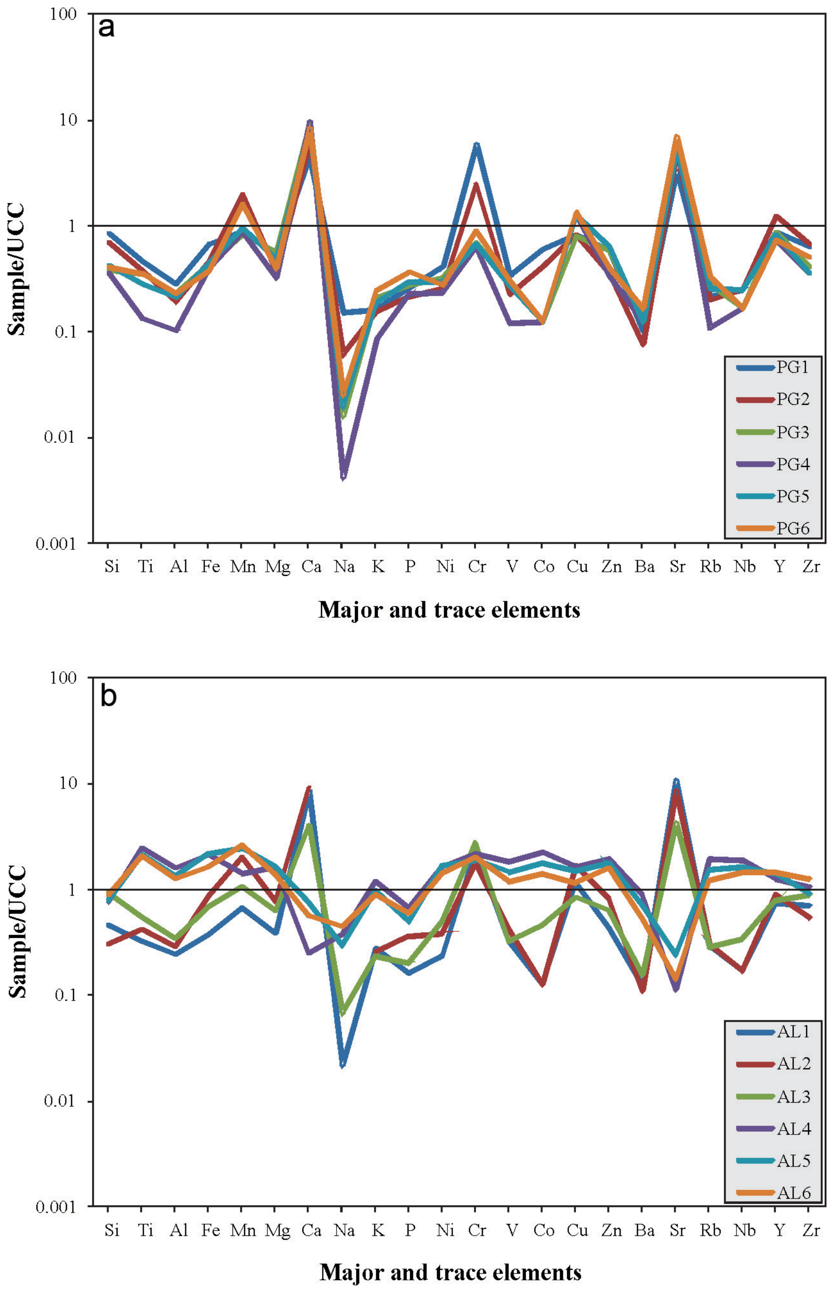

Figure 6. Major and trace elements composition normalized to the UCC (Upper Continental Crust; (McLennan et al., 2006) of the a) calcschist (PG) and b) shale (AL) samples.

DISCUSSION

The mineralogical and petrographic data presented in this study indicate that shales and calcschists from the Frido Unit developed in the deeper parts of the Liguride accretionary wedge, as suggested by the occurrence of aragonite. This is consistent a HP/LT metamorphism due to thermal gradients of 8 °C/km, typical of subduction environments (Spadea, 1976; Knott, 1994; Monaco et al., 1995; Invernizzi et al., 2008; Cavalcante et al., 2012). Such observation is also in agreement with the b_0 value in the Frido Unit metapelites determined by Cavalcante et al. (2012) and with the presence of glaucophane, magnesio-riebeckite, aegirin-augite, phengite and pumpellyite in the Frido Unit metabasites and metadolerites (Beccaluva et al., 1982; Sansone et al., 2011; Sansone and Rizzo, 2012; Sansone et al., 2012a). Several deformation events were recognized within the Frido Unit shales and calcschists involved in the development of brittle, ductile shear zones associated with the onset of tectonic exhumation of the Frido Unit (Vitale et al., 2013).

The geometry of deformation twins and the presence of microstructures in calcite are directly related to the metamorphic grade of the rocks. Calcite of calcschist show bent and spaced straight twins indicate conditions up to 250 °C (Ferril et al., 2004), it's also supported by developed of bulging recrystallization in quartz (Passchier and Trouw, 2005). The occurrence of chlorite, white mica, aragonite and stilpnomelane in the Frido Unit shales and calcschists point toward metamorphic conditions at the high-P and low-T in typical of greenschist conditions. Infact Vitale et al. (2013), within phyllites from the San Severino Lucano area, show the occurence of carpholite and potassic white mica formed at pressures of ~1.2-1.4 GPa and temperatures of "tilde" 350 °C.

Element mobility, source-area weathering and provenance

Geochemical data show that calcium and strontium are positively correlated (*r*=0.84 for the calcschists and *r*=0.96 for the shales), matching the distribution of $CaCO_3$-phases (calcite and aragonite) over the entire studied successions (Figure 7). Mg is depleted relative to the UCC, and is accompanied by the absence of dolomite among the carbonates. In general, Ca shows strong negative correlation with other elements suggesting dilution effects by the carbonates. Aluminum is positively correlated with Ti, Fe, Mg, Na, K and P and most of the trace elements (Figure 7) highlighting as these elements are mainly hosted in the mica-like clay minerals (Mongelli et al., 2006; Perri et al., 2013); furthermore, the positive correlation between Fe and Mg with Al (Figure 7) points out that clay minerals, especially chlorite, play an important role in hosting Mg and Fe.

It is generally accepted that REE, HFSE and Y are largely preserved during regional metamorphism, and thus, can be used to assess the characteristics of the sources (Slack and Stevens, 1994; Girty et al., 1996; Li et al., 2005). The studied samples have K/Rb ratios from 221 to 235 for the calcschists and from 186 to 283 for the shales, slightly higher than the Post-Archean Australian Shale (Taylor and McLennan, 1985), in contrast to the granulite-facies rocks controlled by K-rich minerals or a fluid phase (K/Rb=500-1000, Blein et al., 2003), suggesting that metamorphism did not cause large scale removal of Rb from the protolith.

Among the chemical index of weathering processes, CIA (Chemical Index of Alteration; Nesbitt and Young, 1982) provides a useful measure of the maturity of the sedimentary protolith. The Chemical Index of Alteration is expressed as the molar volumes of [Al/(Al+Ca*+Na+K)] x100, where Ca* represents the CaO only from the silicate fraction (Nesbitt and Young, 1982). As the samples contain some carbonate, CIA' (the molar volumes of [Al/(Al+Na+K)]x100 and, thus, calculated excluding CaO) has been also determined in this study to monitor the source-area weathering (Perri et al., 2014). Both calcschist (mean of CIA=58; mean of CIA'=73) and shale (mean of CIA=70; mean of CIA'=74) samples show low to moderate CIA and CIA' values indicative of low-to-moderate degrees of chemical weathering or a relatively immature source area (Wu et al., 2012). These data are in agreement with those of the Mongelli and Dinelli (2001). Similarly, ICV (Index of Compositional Variability) (Cox et al., 1995) values can be applied to sedimentary rocks in order to determine their compositional maturity. Compositionally, immature sedimentary rocks usually show high ICV values (ICV>1) typical of first-cycle deposits, indicating tendency to occur in tectonically active settings. In contrast, compositionally mature sedimentary rocks usually show low ICV values (ICV<1) typical of recycled deposits and characteristics of tectonically quiescent or cratonic environments (Cox et al., 1995; van de Kamp and Leake, 1985; Perri et al., 2012a). The ICV values of the calcschist (mean=13.3) and shale (mean=4.7) samples are generally higher than 1, indicating low maturity and, thus, first-cycle deposits related to tectonically active settings. Thus, the above mentioned observations suggest that the studied rocks have composite immature sources (Wang et al., 2013). These data are in agreement with those of the Mongelli and Dinelli (2001); in this work similar samples have been studied, showing a simple correlation for the Zr/Sc *vs.* Th/Sc ratios that excludes zircon enrichment and, thus, sediment recycling (Mongelli and Dinelli, 2001). Furthermore, the La-Th-Sc and Th-Sc-Zr/10 plots for similar samples studied by Mongelli and Dinelli (2001), indicate that the sedimentary evolution of the Frido shales is related to a tectonically active setting (Mongelli and Dinelli, 2001), also in agreement with our data from this study.

The distribution of some major and trace elements reflects the source area composition; generally, Fe, Mg, Cr and Ni are related to mafic sources, whereas Al, La and Nb are typical of felsic source. Among these elements, Cr shows high values for some samples of the calcschist suites (PG1 and PG2) and of the shale suites (AL1, AL2 and AL3). Cr among the studied samples may be related to heterogeneous source areas characterized by both felsic and mafic features.

Diagrams based on TiO_2 vs. Al_2O_3 and TiO_2 vs. Ni are commonly used to determine source rock composition. In the TiO_2-Al_2O_3 diagram, mafic (basaltic) and felsic (granitic) source rocks were discriminated (Figure 8); in this plot the studied samples fall between the Basalt+Granite and Granite+Basalt curves suggesting heterogeneous source areas characterized by both felsic and mafic compositions. The latter provenance is also confirmed by the TiO_2 vs. Ni (Figure 8) and fall far from the mature rocks field, supporting the data above shown relative to the immature composition of the studied

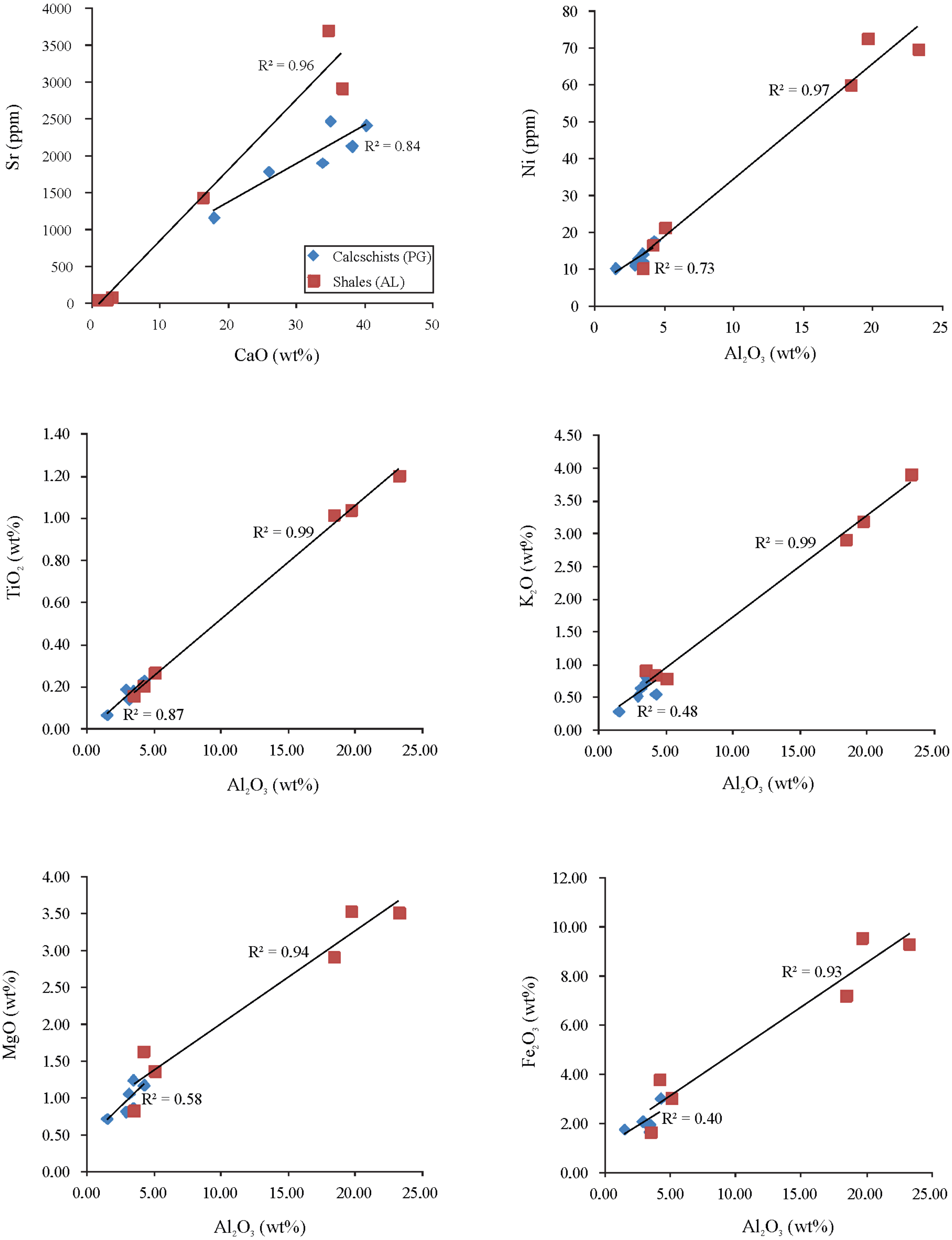

Figure 7. Harker variation diagrams for major and trace elements in calcschist (PG) and shale (AL) samples.

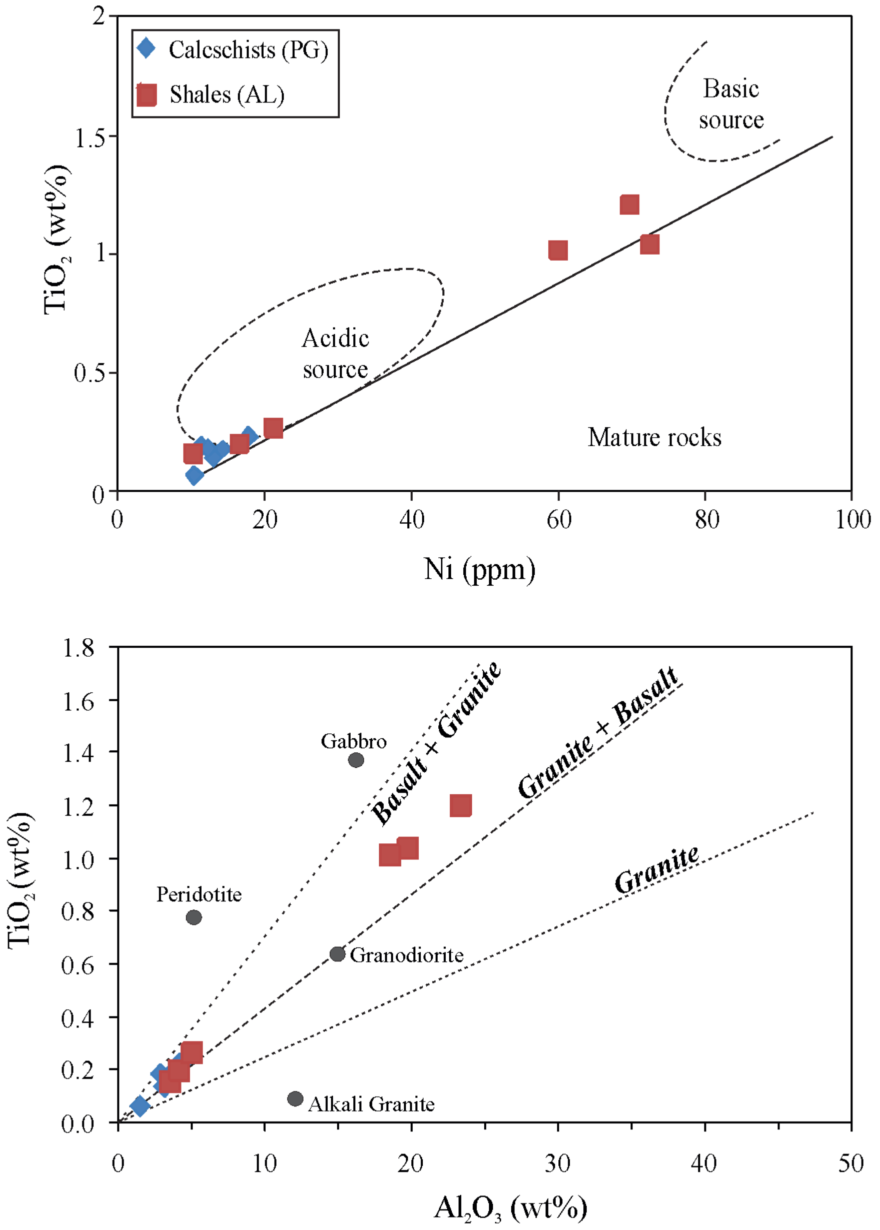

Figure 8. Plots of the TiO_2 vs. Ni and TiO_2 vs. Al_2O_3 ratios, used to determine source rock compositions for the calcschist (PG) and shale (AL) samples.

samples. To infer the source area composition, the Cr/V ratio, an index of the enrichment of Cr over the other ferromagnesian trace elements, is plotted again the Y/Ni ratio, monitoring the general level of ferromagnesian trace elements (Ni) compared to a proxy for HREE (Y) (Perri et al., 2011a and references therein). The Cr/V vs. Y/Ni diagram (Hiscott, 1984) shows trends related to a provenance from ultramafic-to-mefic (high Cr/V ratio) and felsic (low Cr/V and medium-high Y/Ni ratios) rocks (Figure 9). The distribution of the studied samples in this diagram suggests provenance from mixing source(s) of both felsic and mafic compositions, as above mentioned. This is in accordance with a geodynamic contest of the peri-mediterranean area (Laurita et al., 2014), that considers the origin of the Liguride Complex related to thinning and fragmentation within the OCT during Tethyan evolution.

CONCLUSIONS

In this paper we report new data obtained by petrographic, geochemical and mineralogical studies in metasedimentary rocks (shales and calcschists) from the Frido Unit (Liguride Complex). Results allow to better understand the geological processes, source area provenance and tectonic setting of

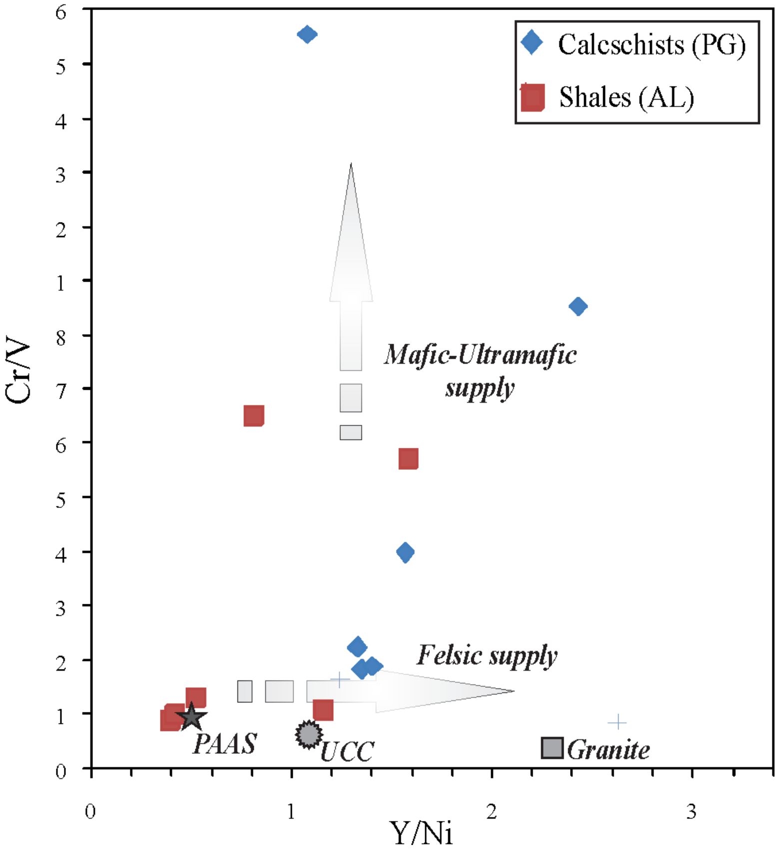

Figure 9. Cr/V vs. Y/Ni ratios (after Hiscott, 1984).

the metasedimenty rocks in the central Mediterranean area.

Petrographic observations show that the Frido Unit shales and calcschists underwent similar HP/LT overprint as testified by the occurrence of aragonite, typical of subduction environments.

According to Cavalcante et al. (2012), different thrust sheets of the Frido Unit underwent fast exhumation after the pressure and temperature peak in the accretionary wedge, with thermal gradients of 8 °C/km.

The Frido Unit shows several deformation events, in the shales characterized by LP/LT conditions, in the calcschists instead by HP/LT conditions, developed during emplacement into the Liguride Complex. In fact the shales of the Frido Unit show metamorphic conditions between anchimetamorfism and greenschist facies, in according to previous authors (Di Leo et al., 2005; Cavalcante et al., 2012; Vitale et al., 2013).

The calcschists of the Frido Unit show greenschist facies metamorphism, also the presence of aragonite indicates that these rocks were affected by HP–LT conditions.

Mineralogical composition of the studied shales and calcschists is closely related to their geochemical variations. In particular, the positive correlation between calcium and strontium matches the distribution of $CaCO_3$-phases (calcite and aragonite) over the entire studied successions, as well as the depletion on Mg relative to the UCC is accompanied by the absence of dolomite among the carbonates. Furthermore, the general negative correlation of Ca with Si, K, Al, Fe and Na suggests dilution effects by the carbonates, whereas the positive correlation of Al with most of the major and trace elements indicates that these elements are mainly hosted in the mica-like clay minerals.

Elemental ratios, such as CIA, CIA' and ICV indices provide useful measures of the maturity of the sedimentary protolith. The CIA and CIA' indices indicate low-to-moderate degrees of chemical weathering or a relatively immature source area. Similarly, ICV indicates low maturity for the studied samples and, thus, first-cycle deposits related to tectonically active settings.

The distribution of some major and trace elements, as shown in the Ti *vs.* Ni and Ti *vs.* Al plots and in the Y/Ni *vs.* Cr/V diagram reflecting the source area composition, mainly suggests heterogeneous sources characterized by both felsic and mafic compositions and, thus, provenance from mixing source(s).

ACKNOWLEDGMENTS

Financial support for this study was provided by University of Basilicata research funds. The authors also wish to thank Prof. R. Cirrincione for his critical review of the manuscript.

REFERENCES

Beccaluva L., Macciotta G., Spadea P. (1982) Petrology and geodynamic significante of the Calabria-Lucania ophiolites. Rendiconti della Società Italiana di Mineralogia e Petrologia 38, 973-987.

Blein O., LaFlèche M.R., Corriveau L. (2003) Geochemistry of the granulitic Bondy gneiss complex: a 1.4 Ga arc in the Central Metasedimentary Belt, Grenville Province, Canada. Precambrian Research 120, 193-217.

Bonardi G., Amore F.O., Ciampo G., De Capoa P., Miconnet P., Perrone V. (1988) Il Complesso Liguride Auct.: stato delle conoscenze e problemi aperti sulla sua evoluzione preappenninica ed i suoi rapporti con l'Arco Calabro. Memorie della Società Geologica Italiana 41**,** 17-35.

Bonardi G., Ciarcia S., Di Nocera S., Matano F., Sgrosso I., Torre M. (2009) Carta delle principali unità cinematiche dell'Appennino meridionale. Nota illustrativa. Italian Journal of Geoscience 128, 47-60.

Bracco J.N., Grantham M.C., Stack A.G. (2012) Calcite growth rates as a function of aqueous calcium-tocarbonate ratio, saturation index, and inhibitor concentration: Insight into the mechanism of reaction and poisoning by strontium. Crystal Growth Design 12, 3540-3548.

Cavalcante F., Belviso C., Laurita S., Prosser G. (2012) P-T constraints from phyllosilicates of the Liguride Complex of the Pollino area (Southern Apennines, Italy): Geological inferences. Ofioliti 37, 65-75.

Cavalcante F., Fiore S., Lettino A., Piccarreta G., Tateo F. (2007) Illite-Smectite mixed layer in Sicilide shales and piggy-back deposits of the Gorgoglione Formation (Southern Apennines): Geological inferences. Bollettino della Società Geologica Italiana 103, 241-254.

Cavalcante F., Belviso C., Finizio F., Lettino A., Fiore S. (2009) Carta geologica delle Unità Liguridi dell'area del Pollino (Basilicata): nuovi dati geologici, mineralogici e petrografici. Regione Basilicata - Dip. Ambiente, Territorio e Politiche della Sostenibilità, 36 pp.

Cello G. and Mazzoli S. (1999) Apennine tectonics in southern Italy: a review. Journal of Geodynamics 27, 191-211.

Cirrincione R. and Monaco C. (1996) Evoluzione tettono-metamorfica dell'Unità del Frido (Appennino Meridionale). Memorie della Società Geologica Italian 51, 83-92.

Cox R., Lowe D.R., Cullers R.L. (1995) The influence of sediment recycling and basement composition on evolution of mudrock chemistry in the southwestern United States. Geochimica Cosmochimica Acta 59, 2919-2940.

Critelli S. (1999) The interplay of lithospheric flexure and thrust accomodation in forming stratigraphic sequences in the southern Apennines foreland basin system, Italy. Memorie dell'Accademia Nazionale dei Lincei 10, 257-326.

Cullers R.L. and Stone J. (1991) Chemical and mineralogical comparison of the Pennsylvanian Fountain Formation, Colorado, U.S.A. (an uplifted continental block) to sedimentary rocks from other tectonic environments. Lithos 27, 115-131.

Cullers R.L., Chaudhuri S., Kilbane N., Koch R.J. (1979) Rare earths in size fractions and sedimentary rocks of Pennsylvanian-Permian age from the mid-continent of the USA. Geochimica Cosmochima Acta 43, 1285-1301.

Cullers R.L., Barrett T., Carlson R., Robinson R. (1987) Rare earth element distributions in size fractions of Holocene soil and stream sediment, Wet Mountains region, Colorado, U.S.A. Chemical Geology 63, 275-297.

Cullers R.L., Basu A., Suttner L. (1988) Geochemical signature of provenance in sand-size material in soils and stream sediments near the Tobacco Root batholith, Montana, U.S.A. Chemical Geology 70, 335-348.

Di Leo P., Schiattarella M., Cuadros J., Cullers R. (2005) Clay mineralogy, geochemistry and structural setting of the ophiolite-bearing units from Southern Italy: a multidisciplinary approach to asses tectonics history and exhumation modalities. Atti Ticinensi di Scienze della Terra 10, 87-93.

Doglioni C, Gueguen E, Harabaglia P, Mongelli F (1999) On the origin of west-directed subduction zones and applications to the western Mediterranean. The Mediterranean basins: Tertiary extension within the alpine orogen. (eds): Durand B, Jolivet L, Horváth F, M Séranne. Special Publications Geological Society, London, 156, pp 541-561.

El Talibi H., Zaghloul M.N., Perri F., Aboumaria K., Rossi A., El Moussaoui S. (2014) Sedimentary evolution of the siliciclastic Aptian-Albian Massylian flysch of the Chouamat Nappe (central Rif, Morocco). Journal African Earth Science 100, 554-568.

Ferril D.A., Morris A.P., Evans M.A., Burkhard M., Groshong R.H., Onash C.M. (2004) Calcite twin morphology: A low temperature deformation geothermometer. Journal of Structural Geology 26, 1521-1529.

Franzini M., Leoni L., Saitta M. (1972) A simple method to evaluate the matrix effects in X-ray fluorescence analysis. X-ray spectrometry 1, 151-154.

Franzini M., Leoni L., Saitta M. (1975) Revisione di una metodologia analitica per fluorescenza X basata sulla correzione degli effetti di matrice. Rendiconti della Società Italiana Mineralogia e Petrologia 31, 365-378.

Girty G.H., Ridge D.L., Knnack C., Johnson D., Al-riyami RK. (1996) Provenance and depositional setting of Paleozoic chert and argillite, Sierra Nevada, California. Journal of Sediment Research 66, 107-118.

Gueguen E., Doglioni C., Fernandez M. (1998) On the post-25 Ma geodynamic evolution of the western Mediterranean. Tectonophysics 298, 259- 269.

Hiscott R.N. (1984) Ophiolitic source rocks for Taconic-age flysch: trace element evidence. Geological Society American Bulletin 95, 1261-1267.

Invernizzi C., Bigazzi G., Corrado S., Di Leo P., Schiattarella M., Zattin M. (2008) New thermobaric constraints of the exhumation history of the Liguride accretionary wedge, Southern Italy. Ofioliti 33, 21-32.

Knott S.D. (1987) The Liguride Complex of Southern Italy - a Cretaceous to Paleogene accretionary wedge. Tectonophysics 142, 217-226.

Knott S.D. (1994) Structure, kinematics and metamorphism in the Liguride Complex, Southern Apennine, Italy. Journal of Structural Geology 16, 1107-1120.

Krumm S. (1996) WINFIT 1.2: version of November 1996 (The

Erlangen geological and mineralogical software collection) of «WINFIT 1.0: a public domain program for interactive profile-analysis under WINDOWS». XIII Conference on Clay Mineralogy and Petrology, Praha, 1994. Acta Universitatis Carolinae Geologica 38, 253-261.

Laurita S. (2009) Il prisma di accrezione liguride affiorante al confine calabro-lucano: studio termocronologico e strutturale. PhD Thesis pp 225.

Laurita S., Prosser G., Rizzo G., Langone A., Tiepolo M., Laurita A. (2014) Geochronological study of zircons from continental crust rocks in the Frido Unit (southern Apennines). International Journal of Earth Science 104, 179-203.

Leoni L. and Saitta M. (1976) X-ray fluorescence analysis of 29 trace elements in rock and mineral standards. Rendiconti della Società Italiana di Mineralogia e Petrologia 32, 497-510.

Li Q.G., Liu S.W., Han B.F., Zhang J., Chu Z.Y. (2005) Geochemistry of metasedimentary rocks of the Proterozoic Xingxingxia complex: implications for provenance and tectonic setting of the eastern segment of the Central Tianshan Tectonic Zone, northwestern China. Canadian Journal of Earth Science 42, 287-306.

Mc Lennan S.M., Hemming D.K., Hanson G.N. (1993) Geochemical approaches to sedimentation, provenance and tectonics. Special Paper-Geological Society of America 284, 21-40.

Mc Lennan S.M., Taylor S.R., Hemming S.R. (2006) Composition, differentiation, and evolution of continental crust: constrains from sedimentary rocks and heat flow: Evolution and Differentiation of the Continental Crust. (eds) Brown M. and Rushmer T., Cambridge University Press, Cambridge, pp 92-134.

Monaco C. and Tortorici L. (1995) Tectonic role of ophiolite-bearing terranes in the development of the Southern Apennines orogenic belt. Terra Nova 7, 153-160.

Monaco C., Tansi C., Tortorici L., De Francesco A.M., Morten L. (1991) Analisi geologico-strutturale dell'Unità del Frido al confine calabro-lucano (Appennino Meridionale). Memorie della Società Geologica Italian 47, 341-353.

Monaco C., Tortorici L., Morten L., Critelli S., Tansi C. (1995) Geologia del versante Nord-orientale del Massiccio del Pollino (Confine calabro lucano). Nota illustrativa sintetica alla scala 1:50.000. Bollettino della Società Geologica Italiana 114, 277-291.

Mongelli G., Critelli S., Perri F., Sonnino M, Perrone V. (2006) Sedimentary recycling, provenance and paleoweathering from chemistry and mineralogy of Mesozoic continental redbed mudrocks, Peloritani Mountains, Southern Italy. Geochemical Journal 40, 197-209.

Mongelli G. and Dinelli E. (2001) The geochemistry of shales from the "Frido unit", Liguride complex, lucanian Apennines, Italy: implications for provenance and tectonic setting". Ofioliti 26, 457-466.

Nesbitt H.W. and Young G.M. (1982) Early Proterozoic climates and plate motions inferred from major element chemistry of lutites. Nature 299, 715-717.

Ogniben L. (1969) Schema introduttivo alla geologia del confine calabro-lucano. Memorie della Società Geologica Italiana 8, 453-763.

Passchier C.W. and Trouw R.A.J. (2005) Microtectonics. Springer-Verlag, Berlin Heidelberg, pp 289.

Patacca E. and Scandone P. (2007) Geology of the southern Apennines. In: Mazzotti A, Patacca E, Scandone P, eds. Results of the CROP Project, Sub-project CROP-04 Southern Apennines (Italy). Bollettino della Società Geologica Italiana, Special Issue 75-119.

Perri F. (2008) Clay mineral assemblage of the Middle Triassic-Lower Jurassic mudrocks from Western-Central Mediterranean Alpine Chains. Periodico di Mineralogia 77, 23-40.

Perri F. (2014) Composition, provenance and source weathering of Mesozoic sandstones from Western-Central Mediterranean Alpine Chains. Journal African Earth Science 91, 32-43.

Perri F., Cirrincione R., Critelli S., Mazzoleni P., Pappalardo A. (2008) Clay mineral assemblages and sandstone compositions of the Mesozoic Longobucco Group (north-eastern Calabria): implication for burial history and diagenetic evolution. International Geology Review 50, 1116-1131.

Perri F., Critelli S., Mongelli G., Cullers R.L. (2011a) Sedimentary evolution of the Mesozoic continental redbeds using geochemical and mineralogical tools: the case of Upper Triassic to Lowermost Jurassic Monte di Gioiosa mudrocks (Sicily, southern Italy). International Journal of Earth Science 100, 1569-1587.

Perri F., Muto F., Belviso C. (2011b) Links between composition and provenance of Mesozoic siliciclastic sediments from Western Calabria (Southern Italy). Italian Journal of Geoscience 130, 318-329.

Perri F., Critelli S., Cavalcante F., Mongelli G., Dominici R., Sonnino M., De Rosa R. (2012a) Provenance signatures for the Miocene volcaniclastic succession of the Tufiti di Tusa Formation, southern Apennines, Italy. Geological Magazine 149, 423-442.

Perri F., Critelli S., Dominici R., Muto F., Tripodi V., Ceramicola S. (2012b) Provenance and accommodation pathways of late Quaternary sediments in the deep-water northern Ionian Basin, southern Italy. Sedimentary Geology 280, 244-259.

Perri F., Critelli S., Martìn-Algarra A., Martìn-Martìn M., Perrone V., Mongelli G., Zattin M. (2013) Triassic redbeds in the Malaguide Complex (Betic Cordillera - Spain): petrography, geochemistry, and geodynamic implications. Earth Science Review 117, 1-28.

Perri F., Borrelli L., Critelli S., Gullà G. (2014) Chemical and minero-petrographic features of Plio-Pleistocene fine-grained sediments in Calabria (southern Italy). Italian Journal of Geosciences 133, 101-115.

Perri F. and Otha T. (2014) Paleoclimatic conditions and paleoweathering processes on Mesozoic continental redbeds from Western-Central Mediterranean Alpine Chains. Palaeogeography, Palaeoclimatology, Palaeoecology 395, 144-157.

Perri F., Caracciolo L., Cavalcante F., Corrado S., Critelli S., Muto F., Dominici R. (2016) - Sedimentary and thermal evolution of the Eocene-Oligocene mudrocks from the southwestern Thrace Basin (NE Greece). Basin Research 28, 319-339.

Piluso E., Cirrincione R., Morten L. (2000) Ophiolites of the Calabrian Peloritan Arc and their relationships with the crystalline basement (Catena costiera and Sila piccola, Calabria Southern Italy). Ofioliti 25, 117-140.

Sansone M.T.C. and Rizzo G. (2009) Rodingites dikes: metasomatism and metamorphism in the Frido Unit (Southern Apennines). Goldschmidt™ 2009 - "Challenges to Our Volatile

Planet” 21-26 Giugno 2009, Davos -Svizzera. Geochimica Cosmochimica Acta Abstracts 73, A1154.

Sansone M.T.C. and Rizzo G. (2010) Rodingites from Frido Unit: evidences for metasomatic alteration. Rendiconti online della Società Geologica Italiana Abstracts 11, 108-109.

Sansone M.T.C. and Rizzo G. (2012) Pumpellyite veins in the metadolerite of the Frido Unit (southern Apennines-Italy). Periodico di Mineralogia 81, 75-92.

Sansone M.T.C., Rizzo G., Mongelli G. (2011) Mafic rocks from ophiolites of the Liguride units (Southern Apennines): petrographical and geochemical characterization. International Geology Review 53, 130-156.

Sansone M.T.C., Tartarotti P., Prosser G., Rizzo G. (2012a) From ocean to subduction: the polyphase metamorphic evolution of the Frido Unit metadolerite dykes (Southern Apennine, Italy). Multiscale structural analysis devoted to the reconstruction of tectonic trajectories in active margins. eds Gosso G., Spalla M.I., Zucali M. Journal Virtual Explorer Electronic Edition 41, Paper 3, doi:10.3809/jvirtex.2011.00289.

Sansone M.T.C., Prosser G., Rizzo G., Tartarotti P. (2012b) Spinel-peridotites of the Frido Unit ophiolites (Southern Apennine-Italy): evidence for oceanic evolution. Periodico di Mineralogia 81, 35-59.

Schettino A. and Turco E. (2011) Tectonic history of the western Tethys since the Late Triassic. Bulletin of the Geological Society of America 123, 89-105.

Slack J.F. and Stevens B.P.J. (1994) Clastic metasediments of the Early Proterozoic Broken Hill Group, New South Wales, Australia: geochemistry, provenance, and metallogenic significance. Geochimica Cosmochimica Acta 58, 257-273.

Spadea P. (1976) I carbonati nelle rocce metacalcaree della Formazione del Frido della Lucania. Ofioliti 1, 431-456.

Spadea P. (1982) Continental crust rocks associated with ophiolites in Lucanian Apennine (southern Italy). Ofioliti 7, 501-522.

Spadea P. (1994) Calabria-Lucania ophiolites. Bollettino di Geofisica e Teorica Applicata 36, 271-281.

Stampfli G.M,. Borel G.D., Marchant R., Mosar J. (2002) Western Alps geological constraints on western Tethyan reconstructions. Journal Virtual Explorer 8, 77-106.

Taylor S.R. and McLennan S.M. (1985) The continental crust: its composition and evolution. Blackwell, Scientific Publication, Carlton, 312 pp.

Tortorici L., Catalano S., Monaco C. (2009) Ophiolite-bearing mélanges in southern Italy. Geological Journal 44, 153-166.

Van de Kamp P.C. and Leake B.E. (1985) Petrography and geochemistry of feldspathic and mafic sediments of the northeastern Pacific margin. Transactions of the Royal Society of Edinburgh. Earth Sciences 76, 411-449.

Vezzani L. (1969) La Formazione del Frido (Neocomiano-Aptiano) tra il Pollino ed il Sinni. Geologica Romana 8, 129-176.

Vitale S., Fedele L., D’Assisi Tramparulo F., Ciarcia S., Mazzoli S., Novellino A. (2013) Structural and petrological analyses of the Frido Unit (southern Italy): New insights into the early tectonic evolution of the southern Apennines-Calabrian Arc system. Lithos 168-169, 219-235.

Wang Z.M., Han C.M., Sua B.X., Sakyi P.A., Malaviarachchi S.P.K., Ao S.J., Wang L.J. (2013) Themetasedimentary rocks fromthe easternmargin of the TarimCraton: Petrology, geochemistry, zircon U–Pb dating, Hf isotopes and tectonic implications. Lithos 179, 120-136.

Wasylenki L.E., Dove P.M., Wilson D.S., De Yoreo J.J. (2005) Nanoscale effects of strontium on calcite growth: An in situ AFM study in the absence of vital effects. Geochimica Cosmochimica Acta 69, 3017- 3027.

Wu G., Chen Y.C., Chen Y.J., Zeng Q.T. (2012) Zircon U–Pb ages of the metamorphic supracrustal rocks of the Xinghuadukou Group and granitic complexes in the Argun massif of the northern Great Hinggan Range, NE China, and their tectonic implications. Journal of Asian Earth Sciences 49, 214-233.